Tool Wear Mechanism and Experimental Study on Deep Hole Gun Drilling of 304 Stainless Steel

JIANG Jitao, LI Liang, SHI Mengting, ZHOU Zilong, WANG Ye*

College of Mechanical Engineering, Yancheng Institute of Technology, Yancheng 224051, P. R. China

(Received 2 December 2024; revised 17 January 2025; accepted 21 January 2025)

Abstract: Deep hole gun drilling is in a closed and semi-closed state, and the machining process is complex. The unstable drilling force, severe tool wear, and poor processing quality have always been difficulties in deep hole gun drilling. 304 stainless steel has good corrosion and heat resistance, and is widely used in various industries. However, high hardness, poor plasticity, and characteristics of sticking knives have always restricted its development in engineering applications. Therefore, this paper uses 304 stainless steel as the research object and performs process parameter optimization and tool wear experiments. Firstly, based on the optimization experiment of process parameters, the influence of cutting speed and feed rate on drilling force and hole wall roughness is analyzed. The process parameters of the subsequent experiment are optimized as follows: spindle speed is 1 270 r / mm, feed rate is 0.02 mm/r, and oil pressure is 3 MPa. Secondly, based on the tool wear experiment, the variation law of tool wear and tool wear form is studied. With the help of scanning electron microscopy (SEM) and energy dispersive spectroscopy (EDS), the tool wear mechanism of deep hole gun drilling 304 stainless steel is expounded. Finally, the influence of tool wear on the processing quality is revealed, and the suggestion of tool regrinding is put forward.

Key words: gun drill; 304 stainless steel; tool wear; processing quality

CLC number: TG52 **Document code:** A **Article ID:** 1005-1120(2025)03-0337-17

0 Introduction

In the mechanical processing industry, deep hole processing demand accounts for about 1/3 of the whole hole processing demand. The demand for processing small-diameter long-deep holes (depth-diameter ratio $\geqslant$ 20) is increasing in the national key development industries, such as aerospace and weapons and equipment. Gun drill processing is a necessary technical means to process small-diameter and long-deep holes[1]. Gun drill consists of three parts: drill bit, drill pipe, and drill handle. The cemented carbide drill bit is matched with the drill pipe rolled from the steel pipe, and the drill bit and drill pipe are connected by seamless welding. The overall structure of the gun drill is shown in Fig.1.

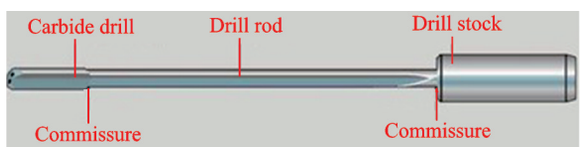

Fig.1 Overall structure of the gun drill

304 stainless steel has excellent corrosion resistance, oxidation resistance, and good mechanical properties. It is widely used in the chemical, food, and construction industries[2]. The main components are shown in Table 1. However, due to the high hardness and wear resistance of 304 stainless steel workpieces, the problem of severe tool wear and shortened life in the machining process is caused[3], which significantly impacts the machining quality of

Table 1 Chemical composition of 304 stainless steel %

Element	Fe	Cr	Ni	C	Mn	Si	S	N
Content	Balance	18—20	8—10.5	0.08	2	1	0.03	0.1

*Corresponding author, E-mail address: jzlliang@163.com.

How to cite this article: JIANG Jitao, LI Liang, SHI Mengting, et al. Tool wear mechanism and experimental study on deep hole gun drilling of 304 stainless steel[J]. Transactions of Nanjing University of Aeronautics and Astronautics, 2025, 42(3): 337-353.

http://dx.doi.org/10.16356/j.1005-1120.2025.03.006

the workpiece. This phenomenon is particularly evident in deep hole processing.

In view of the serious tool wear and low tool life in the machining process, industry scholars have conducted extensive research. Arunkumar et al.[4] used three cooling methods of cutting oil, emulsion, and mist cooling in the study of AISI 1045 deep hole drilling. It was found that the tool wear under mist cooling was 13% — 28% and 25% — 35% lower than that of under cutting oil and emulsion, respectively. It is believed that the reason for this phenomenon is that the abrasive particles and adhesion under mist cooling are reduced. Xu et al.[5] studied the turning of 304 stainless steel. They found that conventional turning would lead to the tool's abrasive wear and adhesive wear, accompanied by deformation and collapse. Adding ultrasonic vibration-assisted turning can significantly improve tool wear. Usman et al.[6] studied the turning of 304 stainless steel micro-textured tools. By comparing the machining quality of ordinary turning tools and micro-textured tools, they found that micro-textured tools could reduce tool wear and improve machining quality to a certain extent. When Xie et al.[7] studied the deep hole gun drilling of 304 stainless steel, they found that the change of the angle between the inner and outer edges of the gun drill had a certain influence on the chip forming and processing quality. Based on this, the angle between the inner and outer edges of the gun drill suitable for processing 304 stainless steel is proposed. Li et al.[8] studied the wear of coated cemented carbide tools with different tooltip radii in turning AISI 321 stainless steel. The results showed that the tool mainly showed abrasive, adhesive, and oxidation wear. Saketi et al.[9] studied the wear mechanism of turning AISI 316L stainless steel with three grades of cemented carbide tools. The results showed that diffusion wear was the main wear mechanism. Fine-grain cemented carbide had a higher crater wear rate, and coarse-grain cemented carbide had a higher flank wear rate. He et al.[10] designed and studied a new multifunctional double-layer AlTiN PVD coatings for turning 304 stainless steel. The research showed that the coating prolonged the tool's service life and reduced the flank face's oxidation wear and diffusion wear. Li et al.[11-13] established a new mechanical model of gun drill and studied the influence of cutting parameters on axial force and torque. The chip fracture mechanism of Ti6Al4V titanium alloy during deep hole gun drilling was studied, which belonged to quasi-cleavage fracture. Abishekraj et al.[14] carried out textured and non-textured tool processing experiments, and found that micro-textured tools could greatly reduce surface roughness and tool wear. Wosniak et al.[15] analyzed the tool wear, drilling torque and chip shape of AISI 4150 low alloy steel during processing. The results showed that there was no adhesive wear on the surface layer tool.

In summary, domestic and foreign research on 304 stainless steel material processing tool wear is mostly for turning processing, and there are few studies on deep hole drilling, especially gun drilling. Therefore, this paper studies the optimization of process parameters and tool wear of 304 stainless steel deep hole gun drilling, optimizes the appropriate process parameters, explores the form and mechanism of tool wear, and expounds the influence of tool wear on the processing quality of 304 stainless steel gun drilling.

1 Main Tool Wear Forms

The primary wear forms of deep hole gun drilling include front and rear tool face wear, tooltip wear, and guide surface wear. In deep hole gun drilling, the tooltip contacts the workpiece first. Owing to the small linear velocity at the tooltip at the initial processing stage, drilling and extrusion co-occur, and the stress concentration occurs. Under the action of a giant drilling force, the tooltip wear is more prominent. With the deepening of the machining process, the inner and outer edges of the gun drill serve as the main cutting task, and the relative sliding between the gun drill and the workpiece causes friction loss. Due to the characteristics of the external chip discharge of the gun drill, there is violent friction between the chip and the front and rear surfaces of the tool. The gun drill bit produces chipping, bonding, and large-area peeling under mechanical, thermal,

and chemical effects. Fatigue spalling and surface ablation appear on the rake face, and evident wear bands appear on the flank face. In the machining process, micro-cracks are generated due to the extrusion friction between the guide surface and the hole wall of the finished workpiece. Under thermal stress fatigue and contact fatigue, wear phenomena such as flake spalling and pits appear, and corresponding wear occurs on the guide surface. The wear form of the gun drill part is shown in Fig.2.

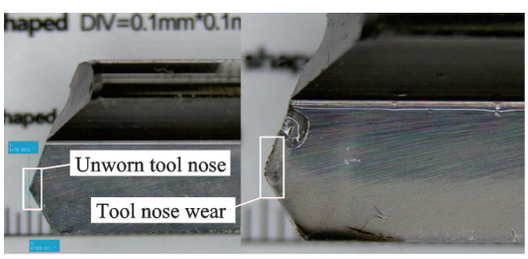

(a) Tooltip wear

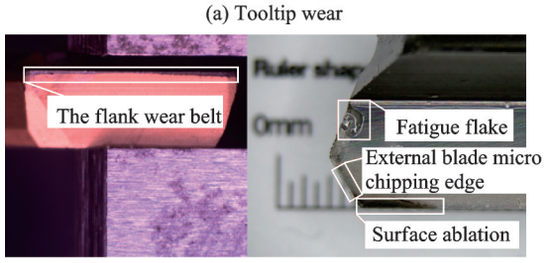

(b) Front and rear tool face wear

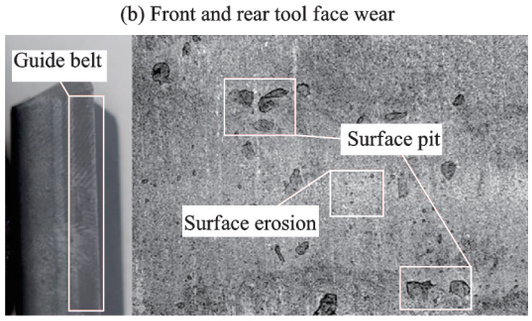

(c) Guide belt wear

Fig.2 Part wear forms of gun drill

2 Determination of Process Parameters of Wear Experiment

2.1 Selection of tools and devices

The tool selected in this experiment is an indexable cutter machine clip gun drill. The length of the gun drill is 1 500 mm, and the diameter is 15 mm. The drill bit comprises a blade and a guide belt that can be freely disassembled. The clamp-type gun drill structure of the indexable cutter-grain machine is shown in Fig.3. The guide belt and blade used in this experiment are shown in Fig.4. The material is KG7015 cemented carbide, and the coating is titanium nitride coating using PVD technology. The blade has high hardness and can complete the deep hole drilling of 304 stainless steel.

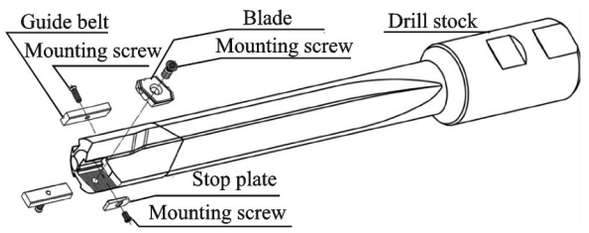

Fig.3 Clamped gun drill with indexable cutter-grain machine

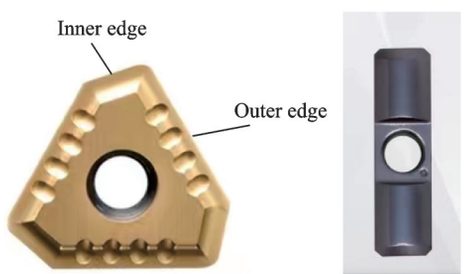

Fig.4 Blade and guide belt

The machine tool used in the experiment is the NCS1600 CNC machine tool. The mechanical data acquisition uses KISTLER 9129AA piezoelectric dynamometer, KISTLER5073A charge amplifier, and HR-426 data acquisition system. The processing equipment is shown in Fig.5, and the equipment installation diagram is shown in Fig.6.

Fig.5 NCS1600 CNC machine tool

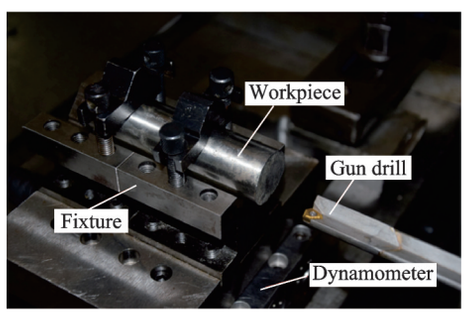

Fig.6 Equipment installation diagram

2.2 Selection of processing parameters

The tool selected in the tool wear experiment is a replaceable gun drill. Since there are few studies on the selection of processing parameters for such gun drills, the variable process parameter experiment is first carried out to determine the optimal processing parameters, which can ensure excellent processing quality and control the tool's wear. The experiment is divided into two groups. The first group is the variable cutting speed experiment, detailed in Table 2. The second group is the variable feed rate experiment, as shown in Table 3.

Table 2 Variable cutting speed experiment

Experimental number	Feed rate f/(mm•r^{-1})	Cutting speed V_c/(m•min^{-1})	Oil pressure p/MPa
1	0.02	40	3
2	0.02	50	3
3	0.02	60	3
4	0.02	70	3
5	0.02	80	3
6	0.02	90	3

Table 3 Variable feed rate experiment

Experimental number	V_c/(m•min^{-1})	f/(mm•r^{-1})	p/MPa
1	60	0.010	3
2	60	0.015	3
3	60	0.020	3
4	60	0.025	3
5	60	0.030	3
6	60	0.035	3

The drilling force in the gun drilling process greatly influences the tool wear and tool life, so the dynamometer is used to measure the axial force throughout the process. At the same time, after the drilling is completed, the workpiece is cut, and the roughness of the hole wall of each section of the workpiece is measured by the surface roughness meter. The measurement data are shown in Table 4.

Table 4 Roughness and drilling force value

Serial number	V_c/(m•min^{-1})	f/(mm•r^{-1})	Roughness Ra/μm	Drilling force F/N
1	40	0.020	0.44	650
2	50	0.020	0.76	600
3	60	0.020	0.58	580
4	70	0.020	0.74	580
5	80	0.020	0.54	550
6	90	0.020	0.42	550
7	60	0.010	0.33	550
8	60	0.015	0.35	580
9	60	0.020	0.44	600
10	60	0.025	0.58	625
11	60	0.030	0.63	650
12	60	0.035	0.82	700

The drilling force in Table 4 are processed and analyzed, and the variation curve of the drilling force with the cutting speed and the variation curve of the drilling force with the feed rate are drawn respectively when the feed rate is constant, as shown in Fig.7 and Fig.8.Fig.7 shows the curve of the drilling force with the cutting speed. It is found that when the feed rate is 0.02 mm/r, the cutting force decreases with the increase of the cutting speed. The drilling force is maintained between 550 N and 650 N in the selected cutting speed range. Fig.8 shows the curve of the drilling force with the feed rate. It is found that when the cutting speed is 60 m/min, the cutting force increases with the increase of the feed rate. The drilling force is maintained between 550 N and 700 N in the selected feed change

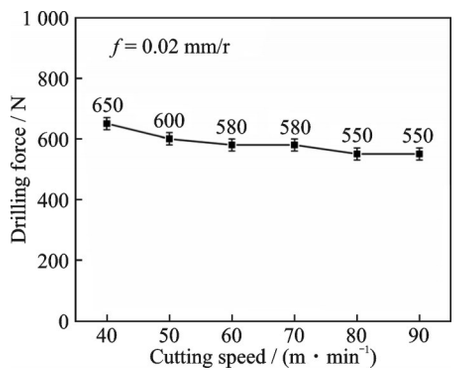

Fig.7 Variation curve of drilling force with cutting speed

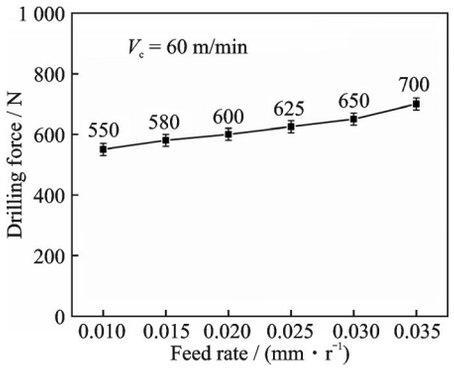

Fig.8 Variation curve of drilling force with feed rate

range.

Based on the roughness in Table 4, the roughness curve with the cutting speed is drawn when the feed rate is constant, and the roughness with the feed rate is drawn when the cutting speed is constant, as shown in Fig.9 and Fig.10, respectively.

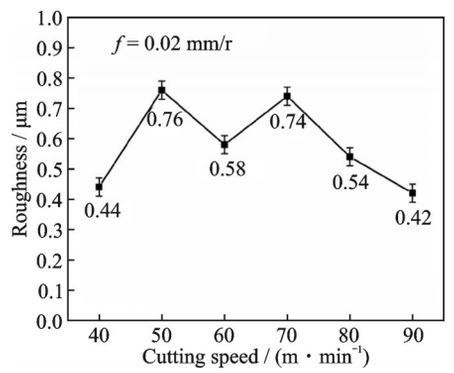

Fig.9 Variation curve of roughness with cutting speed

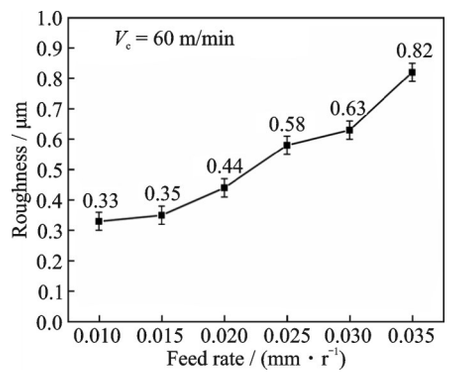

Fig.10 Variation curve of roughness with feed rate

From the analysis of Fig.9, it is found that when the feed rate is kept at 0.02 mm/r, the roughness of the hole wall changes between 0.4 μm and 0.8 μm with the increase of the cutting speed. When the cutting speed is 50 m/min, the hole wall roughness is 0.76 μm, and the hole wall quality is the worst. When the cutting speed is 90 m/min, the hole wall roughness value is 0.42 μm, and the hole wall quality is the best. The roughness of the hole wall tends to decrease with the increase of the cutting speed. From the analysis of Fig.10, it is found that when the cutting speed is kept at 60 m/min, with the increase of the feed rate, the roughness value of the hole wall also increases, and the slope of the curve tends to increase.

According to the above analysis, it is found that the change of the cutting speed has little effect on the roughness of the hole wall, and the drilling force during the machining process is maintained between 550 N and 650 N. The change of the feed rate greatly influences the hole wall roughness and the drilling force. Therefore, the processing parameters of the wear experiment are selected as the cutting speed of 60 m/min, the feed rate of 0.02 mm/r, the spindle speed of the machine tool of 1 270 r/min, and the feed rate of 25 mm/min.

3 304 Stainless Steel Tool Wear Experiment and Analysis

3.1 304 stainless steel tool wear experiment

The wear experiment workpiece is divided into the processing workpiece and the force-measuring workpiece. The processing workpiece is a 304 stainless steel bar with a length of 500 mm and a diameter of 38 mm. The force-measuring workpiece is a 304 stainless steel bar with a length of 100 mm and a diameter of 38 mm. The experiment is carried out by alternating processing and force measurement. The equipment installation diagram is shown in Fig.11.

According to the above variable cutting speed experiment and variable feed rate experiment, the processing parameters of the wear experiment are determined, as shown in Table 5. A total of 15 304 stainless steel bars are processed in the experiment. The cumulative processing length reaches 7 500 mm, and some of the processed workpieces are shown in Fig.12.

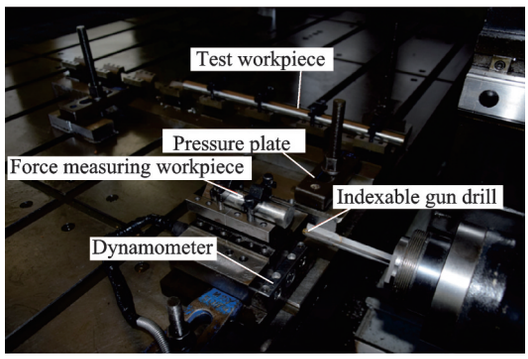

Fig.11 Equipment installation diagram

Table 5 Wear experiment parameter

Spindle speed/ ($r \cdot min^{-1}$)	Feed speed/ ($mm \cdot min^{-1}$)	f/($mm \cdot r^{-1}$)	p/MPa
1 270	25	0.02	3

Fig.12 Processed workpieces

3.2 Analysis of worn form of rake face and flank face

The grinding degree of the tool is observed and analyzed by an electron microscope. Fig.13 is the state diagram of the blade without processing. It is found that when the processing has not yet begun, the front and rear surfaces of the blade are smooth and there are no scratch. The coating on the tool's surface is evenly distributed without apparent damage, and the internal and external cutting edges are sharp and shiny.

Fig.14 shows partial wear state diagrams of the rake face of the outer cutting edge under different machining hole depths. It is found that there are many fatigue spalling phenomena on the rake face of the outer cutting edge. In the early processing stage, when the cumulative processing hole depth is below 3 500 mm, the outer edge rake face appears to have a point spalling phenomenon, and the spalling range is concentrated on the blade's edge. With

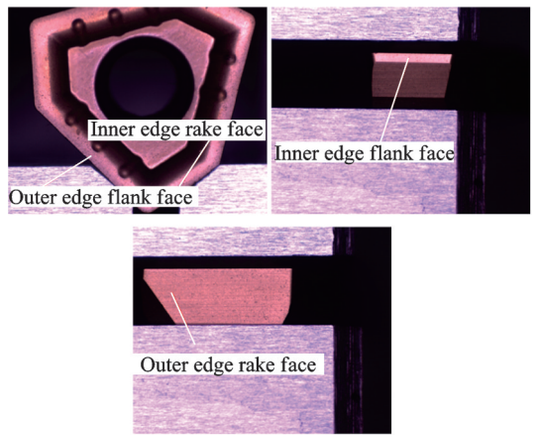

Fig.13 Blade state without processing

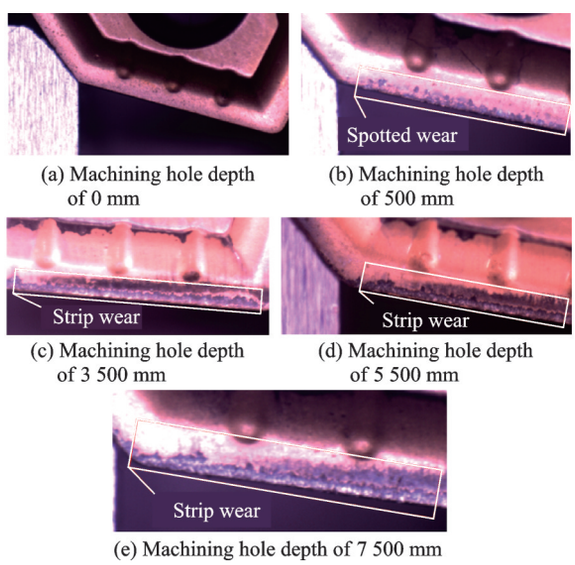

Fig.14 Partial wear state diagrams of outer edge rake face

the continuous increase of the cumulative depth of the machining hole, the spalling area of the rake face of the outer edge is increasing. The phenomenon of point spalling becomes strip spalling and gradually spreads to the inside of the blade. Because the outer cutting edge of the replaceable gun drill is longer than the inner cutting edge, the force at the outer cutting edge is more significant than that at the inner cutting edge. The friction between the rake face of the outer cutting edge and the workpiece is more severe, resulting in many fatigue spalling phenomena.

Fig.15 shows partial wear state diagrams of the rake face of the inner cutting edge under different machining hole depths. It is found that there is a large area of surface ablation on the rake face of the inner cutting edge, and the surface burning area in-

creases with the continuous increase of the machining depth. Due to the severe friction between the tool and the workpiece during the machining process, a local high-temperature environment is formed. Even under the cooling effect of the high-pressure cutting fluid, there is still a large amount of cutting heat residue, resulting in extensive surface ablation on the rake face of the internal cutting edge.

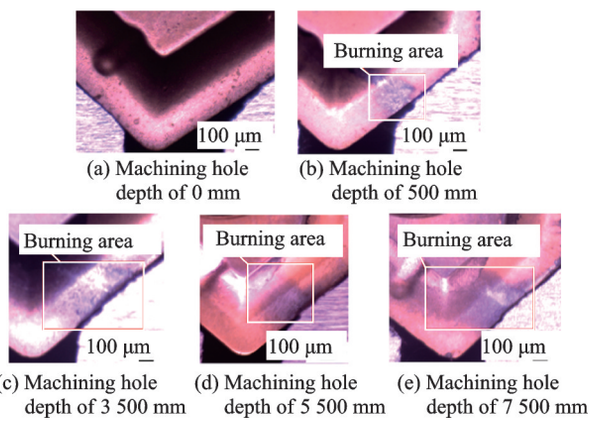

Fig.15 Partial wear state diagrams of inner edge rake face

Fig.16 shows partial wear state diagrams of the outer cutting edge flank surface under different machining hole depths. It is found that the flank surface of the outer cutting edge appears to fatigue spalling and surface ablation. In the early stage of machining, when the hole depth is 500 mm, the surface ablation phenomenon occurs on the flank of the outer cutting edge, and the burning phenomenon is mainly concentrated near the tooltip. At the same time, a small amount of fatigue spalling occurs at the outer cutting edge. With the increase of the depth of the machining hole, there is no noticeable increase in the burning area on the flank surface of the outer cutting edge. When the cumulative depth of the machining hole reaches 3 500 mm, the flank surface of the outer cutting edge appears to be stripped off, and a transparent wear band is formed. With the increase of the cumulative processing depth, the range of wear bands becomes larger and larger, and the degree of fatigue spalling becomes more serious.

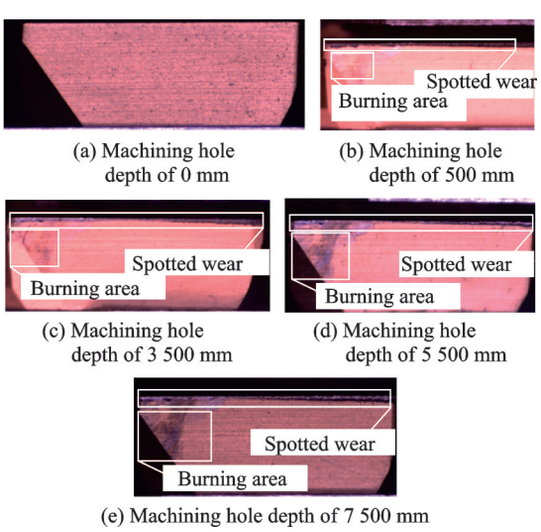

Fig.16 Partial wear state diagrams of outer cutting edge flank face

Fig.17 shows partial wear state diagrams of the inner cutting edge flank surface under different machining hole depths. When the hole depth is 500 mm, a small amount of fatigue spalling occurs on the flank surface of the inner cutting edge. As the depth of the machining hole increases, the wear of the flank face of the inner edge changes little. When the machining hole depth reaches 7 500 mm, it can be found that a clear wear band appears on the flank face of the inner cutting edge. Therefore, in the deep hole gun drilling of 304 stainless steel, the rake face of the inner and outer cutting edges mainly appears to be fatigue spalling and surface ablation. The worn form of the rake face of the outer

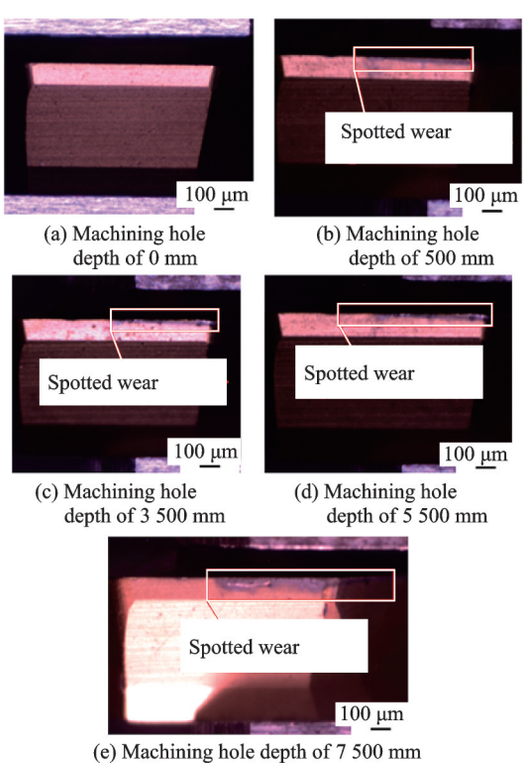

Fig.17 Partial wear state diagrams of inner cutting edge flank face

cutting edge is mainly fatigue spalling, the worn form of the rake face of the inner cutting edge is mainly surface ablation, and the worn form of the flank face of the inner and outer cutting edges is mainly fatigue spalling.

3.3 Analysis of tool wear loss

The image view image processing software measures the wear of the rake and flank surfaces of the tool's cutting edge. The measured data are shown in Table 6.

Table 6 Tool wear

Serial number	Machining hole depth/mm	Wear amount of outer edge rake face/mm	Burning area of inner edge rake face/ mm^2	Wear amount of outer edge flank face/mm	Burning area of outer edge flank face/mm^2	Wear amount of inner edge flank face/mm
1	500	0.152	0.456	0.051	0.315	0.044
2	2 000	0.161	0.481	0.053	0.331	0.058
3	3 500	0.362	0.601	0.064	0.332	0.057
4	5 000	0.381	0.591	0.077	0.342	0.061
5	6 500	0.398	0.649	0.078	0.347	0.065
6	7 500	0.462	0.749	0.087	0.371	0.132

Fig.18 shows the variation curves of tool wear with machining hole depth. It is found that the wear amount of the rake face of the inner and outer cutting edges increases with the increase of machining hole depth. The wear amount of the rake face of the outer cutting edge is always more significant than that of the flank face of the outer cutting edge and the inner cutting edge. The wear on the flank face has maintained a steady growth trend. When the machining hole depth reaches 6 000 mm, the flank face of the inner cutting edge begins to aggravate wear. The wear of the rake face is pronounced. When the machining hole depth reaches 3 500 mm, the rake face is severely worn, and the wear amount reaches 0.35 mm. Fig.19 shows the variation curves of the tool burning area with the change of machining hole depth. It is found that the burning area of the rake face of the inner cutting edge is always more significant than that of the flank face of the outer cutting edge. With the increase of machining hole depth, the burning area of the flank surface of the outer cutting edge has continuously and steadily increased. The burning area of the rake face of the inner cutting edge increases sharply to 0.6 mm^2 when the machining hole depth reaches 3 500 mm. When the final machining hole depth reaches 7 500 mm, the burning area of the rake face of the inner cutting edge reaches 0.75 mm^2.

Therefore, the edge wear of the replaceable gun drill is mainly reflected on the rake face and the flank face. The maximum width of the wear band on the rake face of the outer edge can reach 0.46 mm, and the width of the wear band on the flank face of the outer edge and the flank face of the inner edge is within 0.1 mm. The maximum ablation area on the rake face of the inner edge can reach 0.74 mm^2, and the ablation area on the flank face of the outer edge is maintained at about 0.33 mm^2. Through the above analysis, it is found that tool wear is mainly divided into two stages: normal wear (Machining hole depth$\leqslant$3 500 mm) and severe wear (Machining hole depth$>$3 500 mm). In the early drilling stage, because the outer cutting edge undertakes the main cutting task, a small amount of wear occurs on the outer cutting edge's rake face and flank face. Due to the influence of drilling heat, a small amount of sur-

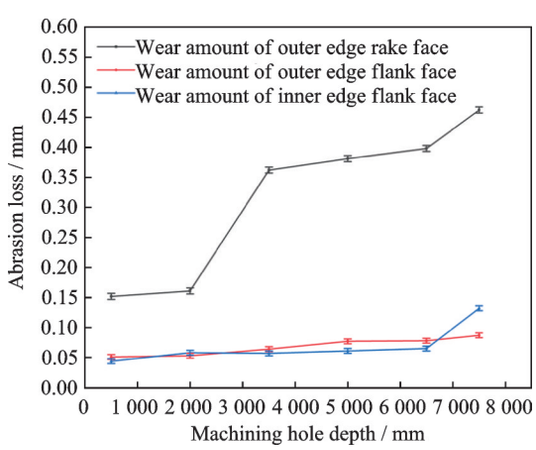

Fig.18 Variation curves of tool wear with machining hole depth

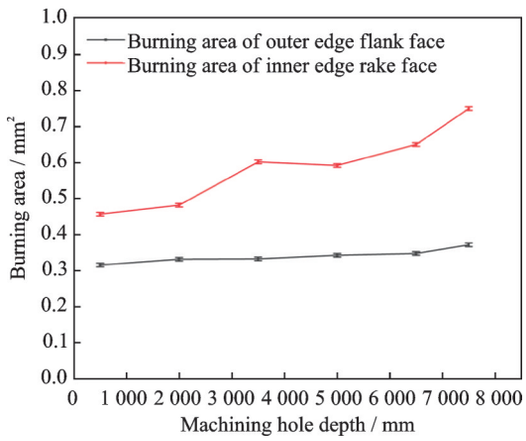

Fig.19 Variation curves of tool burning area with machining hole depth

face ablation occurs on the inner cutting edge's rake face and flank face. With the increase of drilling depth, when the cumulative machining hole depth reaches 3 500 mm, the tool wears violently, a large number of fatigue spalling occurs on the rake face of the outer cutting edge, and a large area of ablation occurs on the rake face of the inner cutting edge.

3.4 Analysis of tool wear mechanism of rake and flank faces

In order to study the wear mechanism of the tool's rake face and flank face, the Nova Nano SEM 450 field emission scanning electron microscope (SEM) is used to scan and analyze the wear of the rake face and flank face. The use of the equipment is shown in Fig.20.

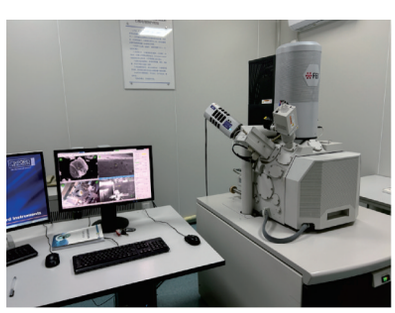

Fig.20 Nova Nano SEM 450 field emission scanning electron microscope

Fig.21 shows the energy dispersive spectroscopy (EDS) analysis results of the unprocessed part of the tool. It is found that the titanium nitride coating on the surface of the tool is complete. The coating has the characteristics of high hardness, good

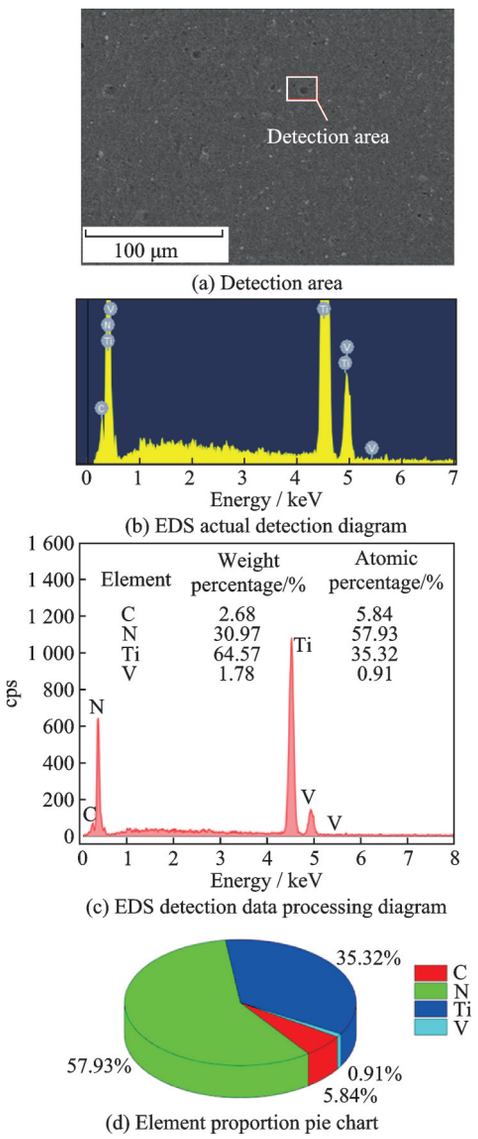

Fig.21 EDS analysis results of unprocessed part of the tool

wear resistance, and low friction coefficient and has a particular protective effect on the tool.

Fig.22 is the SEM morphology of the outer cutting edge rake face. It is found that after processing, a small number of pits are formed by coating peeling, and a large number of binders appear on the rake face of the outer cutting edge of the tool. Fig.23 shows EDS analysis result diagrams of the outer cutting edge rake face. Compared with the EDS analysis result diagrams of the unprocessed tool, it is found that O, Si, and Fe elements appear, among which O atom accounts for 13.44%, Fe atom accounts for 7.49%, and Si atom accounts for 0.56%. Because the elements in the tool and coating react with O atoms in the air to form oxides, the proportion of O atoms increases. The in-

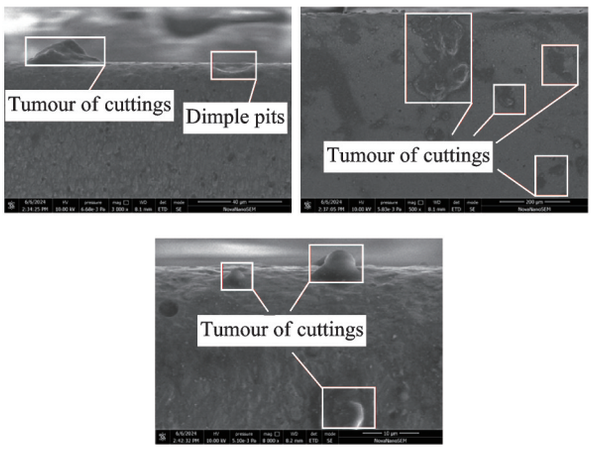

Fig.22 SEM morphology of rake face of outer cutting edge

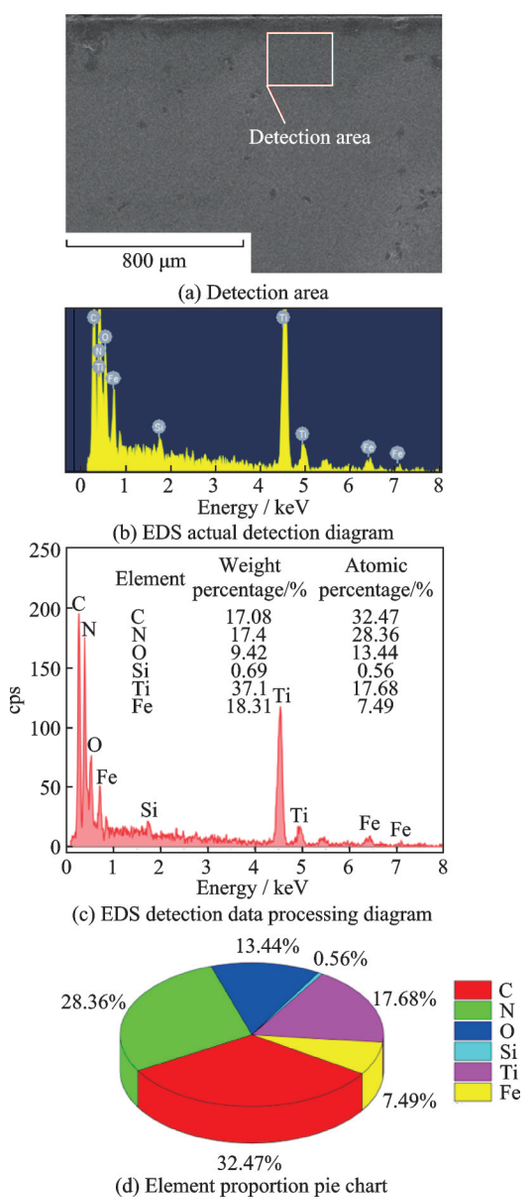

Fig.23 EDS analysis results of rake face of outer cutting edge

crease in the proportion of Fe and Si atoms is due to the diffusion of elements from the workpiece 304 stainless steel into the tool matrix. Therefore, the rake face of the outer cutting edge of the tool mainly causes adhesive wear, oxidation wear, and diffusion wear during the machining process.

Fig.24 is the SEM morphology of the inner cutting edge rake face. It is found that after processing, a large area of coating peeling and more binders are found on the rake face of the inner cutting edge of the tool. Furrows of different depths and craters can be seen at the peeling of the coating. Fig.25 shows EDS analysis result diagrams of the inner cutting edge rake face. Compared with the EDS analysis result diagrams of the unprocessed tool, it is found that O, Cr, and Fe elements appear, among which O atom accounts for 19.28%, Fe atom accounts for 1.85%, and Cr atom accounts for 0.84%. Because the elements in the tool and coating react with O atoms in the air to form oxides, the proportion of O atoms increases. The increase in the proportion of Fe and Cr atoms is due to the diffusion of the elements in the 304 stainless steel into the tool matrix. Therefore, the worn forms of the rake face of the internal cutting edge during the machining process are mainly adhesive wear and oxidation wear, accompanied by a small amount of diffusion wear; when the coating on the rake face of the inner cutting edge peels off, abrasive wear becomes the leading cause of tool wear.

Fig.26 is the SEM morphology of the outer cutting edge flank surface. It is found that after processing, a prominent wear zone and some binders are

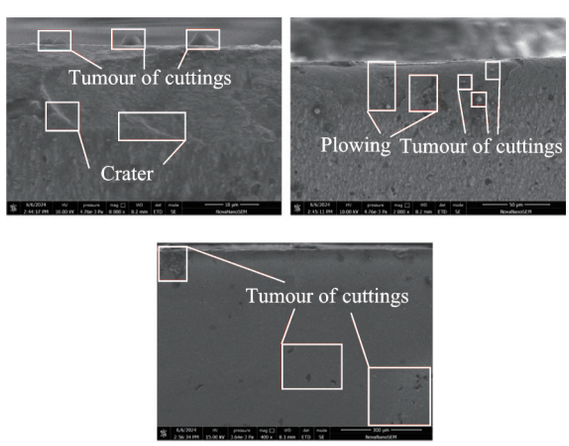

Fig.24 SEM morphology of rake face of inner cutting edge

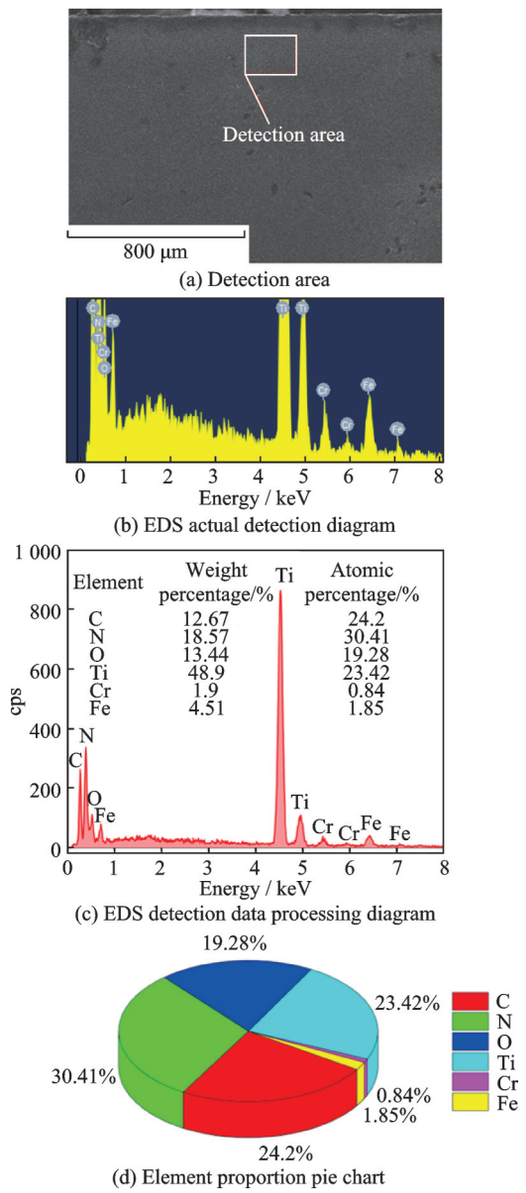

Fig.25 EDS analysis results of rake face of inner cutting edge

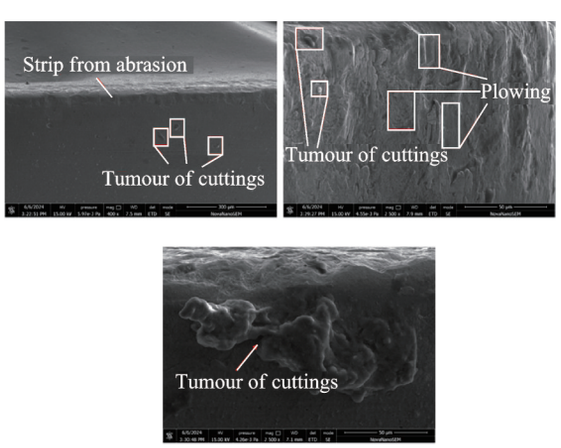

Fig.26 SEM morphology of outer cutting edge flank face

found on the flank surface of the outer cutting edge of the tool. Coating peeling and furrows of different depths can be seen in the war zone. Fig.27 shows EDS analysis results of the flank face of the outer cutting edge. Compared with the EDS analysis results of the unprocessed tool, it is found that O, Si, S, Cr, Mn, and Fe elements appear, among which O atom accounts for 32.98%, Si atom accounts for 0.93%, S atom accounts for 0.36%, Cr atom accounts for 1.8%, Mn atom accounts for 0.62%, and Fe atom accounts for 1.02%. Because the elements in the tool and coating react with O atoms in the air to form oxides, the proportion of O atoms continues to increase. The increase in the proportion of Fe, Cr, Si, S, and Mn atoms is due to the diffu-

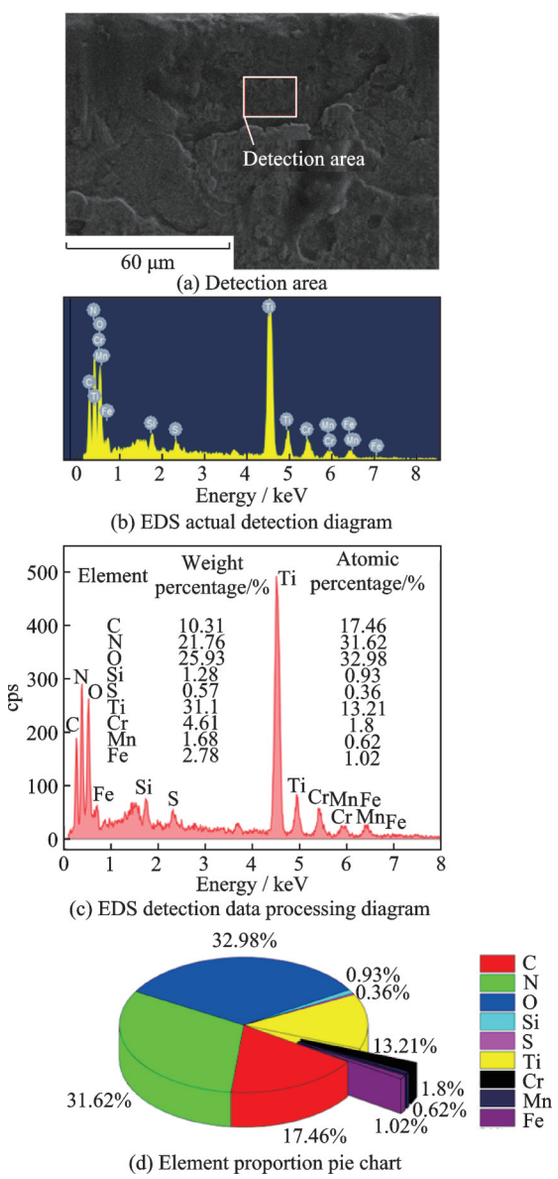

Fig.27 EDS analysis results of flank face of outer cutting edge

sion of the elements in the 304 stainless steel into the tool matrix. Therefore, the worn form of the flank face of the outer cutting edge during the machining process is mainly abrasive wear and oxidative wear, accompanied by a small amount of diffusion wear and adhesive wear.

Fig.28 is the SEM morphology of the inner cutting edge flank face. It is found that after processing, a large area of coating peeling occurs on the flank face of the inner cutting edge of the tool, and a large number of binders and some furrows of different depths appear on the tool substrate. Fig. 29 shows EDS analysis result diagrams of the inner cutting edge flank face. Compared with the EDS analysis result diagrams of the unprocessed tool, it is found that O, Cr, and Fe elements appear, among which O atom accounts for 14.89%, Cr atom accounts for 0.87%, and Fe atom accounts for 1.64%. Because the elements in the tool and coating react with O atoms in the air to form oxides, O atoms' proportions increase. The increase in the proportion of Fe and Cr atoms is due to the diffusion of elements from the workpiece 304 stainless steel into the tool matrix; the sharp increase in the proportion of N atom is due to the diffusion of N atom in the coating into the tool matrix during high-temperature processing. Therefore, the flank face of the internal cutting edge is mainly dominated by adhesive wear, abrasive wear, and oxidation wear during the machining process, accompanied by a small amount of diffusion wear.

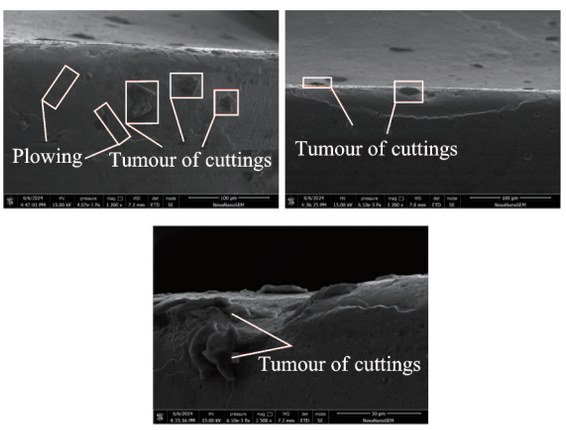

Fig.28 SEM morphology of flank face of inner cutting edge

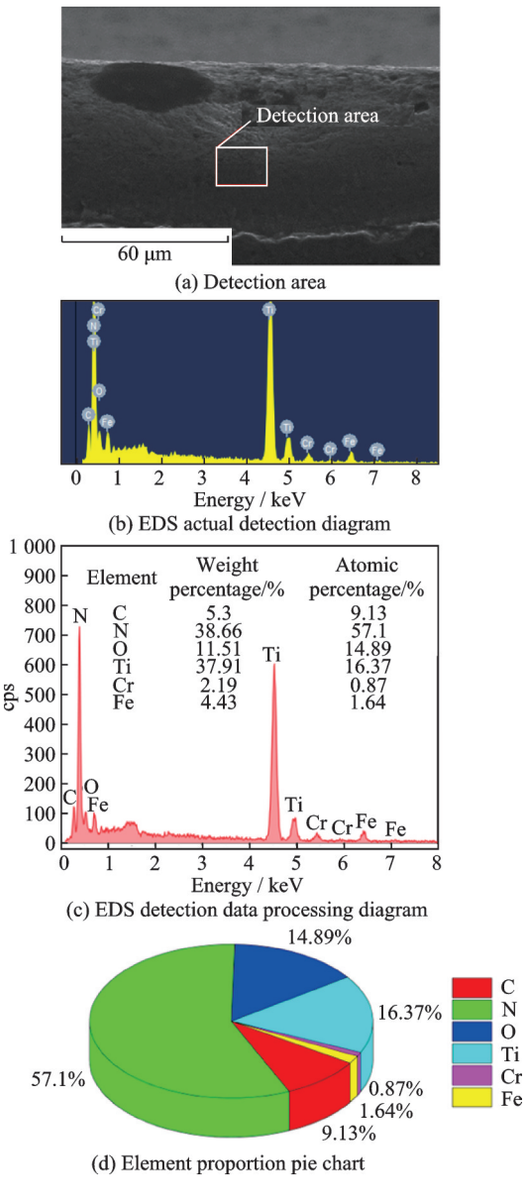

Fig.29 EDS analysis results of flank face of inner cutting edge

4 Analysis of Influence of Tool Wear on Machining Quality

4.1 Effect of tool wear on drilling force

A total of 15 bars are processed in the wear experiment, with a total processing depth of 7 500 mm. A total of 15 sets of axial drilling force data are collected, as shown in Table 7. And the curve of drilling force with machining hole depth is shown in Fig. 30. Fig.30 shows the curve of the drilling force changing with the depth of gun drilling. Due to the existence of cylinder ejection pressure in the actual processing, it is about 500 N. Therefore, the initial cylin-

Table 7 Drilling force of 15 bars with different machining hole depth

Serial number	Machining hole depth/mm	Drilling force /N	Serial number	Machining hole depth/mm	Drilling force/N
1	500	570	9	4 500	640
2	1 000	575	10	5 000	650
3	1 500	575	11	5 500	655
4	2 000	580	12	6 000	680
5	2 500	580	13	6 500	700
6	3 000	580	14	7 000	750
7	3 500	600	15	7 500	800
8	4 000	600			

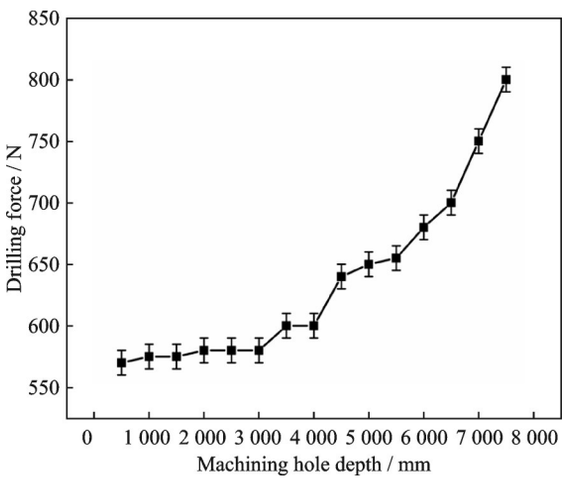

Fig.30 Curve of drilling force changing with machining hole depth

der force must be subtracted when drawing the change curve. The curve's analysis shows that the drilling force is stable at about 570 N due to the slight wear of the tool in the early stage of drilling. With the continuous increase of the drilling depth, when the cumulative reaches 3 500—4 000 mm, the tool wear gradually increases and the drilling force increases to 650 N. The tool wear increases sharply when the drilling depth reaches 7 500 mm and the drilling force reaches about 800 N. Therefore, with the increase of drilling depth, the tool wear becomes more severe, leading to the increase of axial drilling force.

4.2 Effect of tool wear on roughness

A total of 15 bars are processed in the wear experiment, with a total processing depth of 7 500 mm. The roughness meter is used for measurement, and 15 sets of roughness data are collected. The use of the equipment is shown in Fig.31. In the measurement, the entrance section, middle section, and exit section of each workpiece are tested, and the collected data are shown in Table 8. The curves of

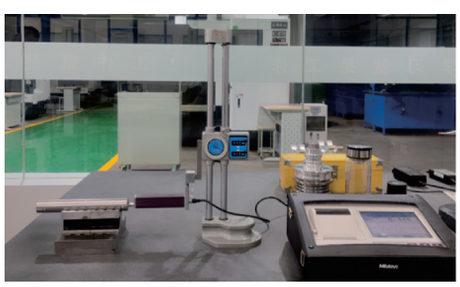

Fig.31 Roughness meter usage diagram

Table 8 Roughness of machined workpieces

Number of borehole	Machining hole depth/mm	Roughness at the entrance/μm	Roughness of intermediate section/μm	Roughness at the outlet/μm
1	500	0.44	0.21	0.32
2	1 000	0.38	0.19	0.29
3	1 500	0.42	0.26	0.34
4	2 000	0.47	0.32	0.35
5	2 500	0.43	0.21	0.37
6	3 000	0.55	0.29	0.41
7	3 500	0.58	0.27	0.44
8	4 000	0.72	0.31	0.48
9	4 500	0.63	0.33	0.47
10	5 000	0.82	0.39	0.62
11	5 500	0.76	0.37	0.56
12	6 000	0.88	0.42	0.59
13	6 500	0.96	0.49	0.72
14	7 000	1.15	0.72	0.86
15	7 500	1.28	0.88	0.96

roughness with the machining hole depth are shown in Fig.32.

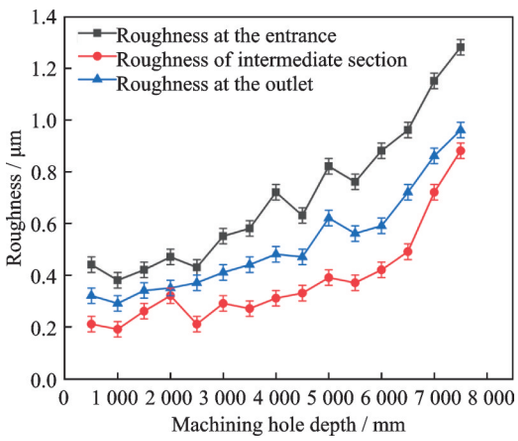

Fig.32 Curves of roughness changing with machining hole depth

Fig.32 is the curves of roughness changing with the machining hole depth. It is found that the roughness value of the workpiece increases with the increase of the processing depth. The roughness at the entrance is always more significant than that of the intermediate section and the outlet, and the roughness of the intermediate section is the smallest. Due to the tooltip at the entrance being in direct contact with the workpiece, the contact area between the tool cutting edge and the workpiece is small, and the tool has some vibration, resulting in higher surface roughness. As the drill bit ultimately enters the workpiece, the tool's cutting edge is completely in contact with the workpiece, the processing reaches a stable state, and the surface roughness reduces compared with the entrance. When the workpiece is drilled through, the contact area between the tool's cutting edge and the workpiece gradually decreases, the tool vibrates again, and the roughness improves slightly. When the cumulative machining hole depth is less than 3 500 mm, the tool wear is better, and the surface roughness of the workpiece maintains a stable numerical fluctuation. With the increase of the machining hole depth, the tool wear is gradually severe, and the roughness increases. When the cumulative machining hole depth reaches 5 500 mm, the tool wears violently, and the roughness of the hole wall increases sharply.

4.3 Effect of tool wear on straightness

A total of 15 bars are processed in the wear experiment, with a total processing depth of 7 500 mm, and 15 sets of straightness data are collected. Through the three-coordinate measuring instrument, the five-point method fits the coordinate value of the hole's center point. Then, a data set is measured every 100 mm, and each processing bar is measured at five straightness values. The data collected are shown in Table 9. The straightness error curves of different machining hole depths are shown in Fig.33. The straightness error curve with the cumulative processing depth is shown in Fig.34.

Table 9 Measured values of workpiece straightness error

Serial number	Machining hole depth/mm	Measurement point					
		0 mm	87 mm	188 mm	288 mm	388 mm	488 mm
1	500	0	0.002 0	0.003 7	0.001 8	0.004 4	0.003 5
2	1 000	0	0.003 1	0.002 1	0.001 9	0.002 8	0.003 1
3	1 500	0	0.002 6	0.001 3	0.001 8	0.001 2	0.001 9
4	2 000	0	0.002 8	0.001 9	0.002 3	0.002 8	0.003 2
5	2 500	0	0.003 3	0.003 1	0.002 9	0.003 8	0.003 5
6	3 000	0	0.003 1	0.004 2	0.004 9	0.004 7	0.005 1
7	3 500	0	0.005 8	0.004 9	0.005 2	0.006 3	0.007 7
8	4 000	0	0.007 8	0.007 7	0.014 3	0.017 6	0.018 8
9	4 500	0	0.008 2	0.006 9	0.009 8	0.019 3	0.017 8
10	5 000	0	0.012 0	0.011 2	0.015 1	0.019 2	0.019 9
11	5 500	0	0.013 2	0.012 9	0.017 2	0.021 1	0.021 7
12	6 000	0	0.015 3	0.013 3	0.018 4	0.019 2	0.022 3
13	6 500	0	0.016 9	0.021 1	0.020 2	0.021 9	0.023 8
14	7 000	0	0.019 5	0.020 1	0.021 9	0.023 8	0.031 4
15	7 500	0	0.024 1	0.019 8	0.025 7	0.024 1	0.032 8

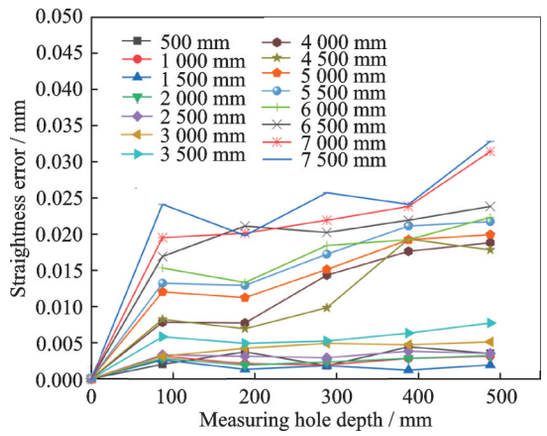

Fig.33 Straightness error variation curves at different processing depths

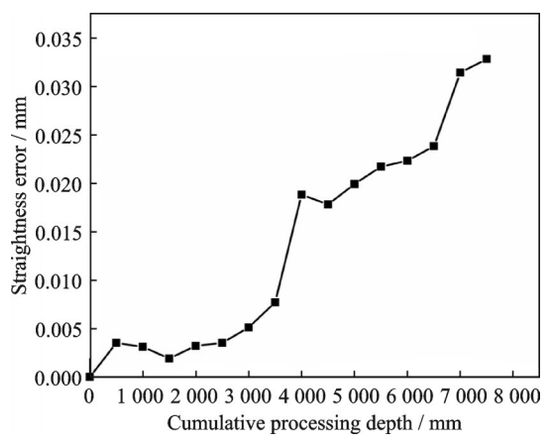

Fig.34 Straightness error change curve with the cumulative processing depth

From Fig.33, it is found that when the machining hole depth is below 3 500 mm, the straightness error of the workpiece fluctuates little and is in a relatively stable state. With the increase of machining hole depth, the fluctuation range of the straightness error becomes larger and larger. When the machining hole depth reaches 7 500 mm, the fluctuation of straightness error is the largest. Through the analysis of graphic changes in Fig.34, it is found that when the cumulative machining hole depth is less than 3 500 mm, the straightness error fluctuates, but it is less than 0.007 7 mm. At this time, the tool wear has little effect on the straightness. When the cumulative machining hole depth is 4 000 — 6 500 mm, the influence of tool wear on machining quality increases gradually, and the straightness error fluctuates between 0.02 mm and 0.03 mm. When the cumulative machining hole depth exceeds 7 000 mm, the tool wears violently, the straightness error increases sharply, and the maximum straightness error reaches 0.032 8 mm.

5 Conclusions

The process parameter optimization experiment and tool wear experiment of 304 stainless steel processed by interchangeable gun drill are carried out. The influences of different process parameters and tool wear on drilling force, hole wall roughness, and machining hole straightness is analyzed. The form and mechanism of tool wear are studied, and the following conclusions are drawn:

(1) Based on the optimization experiment of process parameters, the influences of cutting speed and feed rate on the drilling force and the hole wall roughness are obtained. The drilling force decreases with the increase of cutting speed and increases with the increase of feed rate. The roughness of the hole wall increases with the increase of the feed rate. Changing the cutting speed has little effect on the roughness of the hole wall, and the roughness remains in the range of 0.4—0.8 μm. Based on this, the process parameters of the subsequent experiment are optimized as the cutting speed of 60 m/min and the feed rate of 0.02 mm/r.

(2) Tool wear has apparent stage division: normal wear (Machining hole depth ≤ 3 500 mm) and sharp wear (Machining hole depth > 3 500 mm). In these two stages, the wear amount of the rake face of the outer edge is always more significant than that of the flank face of the outer edge and the flank face of the inner edge, and the maximum wear band width can reach 0.46 mm. The burning area of the rake face of the inner edge is always more extensive than that of the flank face of the outer edge, and the maximum can reach 0.74 mm^2. Due to the wear amount of the outer blade rake face increases sharply in the severe wear stage, and the wear amount is always greater than 0.35 mm. Combined with the measurability of various parameters of the tool, it is recommended to the maximum wear of the outer edge rake face as the basis for the regrinding the gun drill. The tool wear mechanism is as fol-

lows: When the tool coating is intact, it is mainly adhesive wear and oxidative wear, accompanied by a small amount of diffusion wear, among which the diffusion wear of the rake face of the outer cutting edge is the most serious. After a large number of the tool coating peelings off, the wear mechanism of the tool substrate is mainly adhesive wear, abrasive wear, and oxidation wear, accompanied by a small amount of diffusion wear.

(3) The drilling force increases with the increase of tool wear. In the normal wear stage, the drilling force is stable at about 570 N; in the sharp wear stage, the drilling force can reach about 800 N. The roughness of the hole wall increases with the increase of tool wear. In the normal wear stage, the roughness of the hole wall fluctuates at 0.25 μm; in the sharp wear stage, the increased trend of roughness becomes more prominent, and the maximum can reach 0.8 μm. The straightness error increases with the increase of tool wear. In the normal wear stage, the straightness error of the workpiece fluctuates less, the error is below 0.007 7 mm, and the processing quality is higher. With the continuous increase of processing depth, the fluctuation range of the straightness error is getting larger and larger. When the processing depth reaches 7 500 mm, the straightness error fluctuates the most, reaching 0.032 8 mm.

Reference

[1] TNAY G L, WAN S, WOON K S, et al. The effects of dub-off angle on chip evacuation in single-lip deep hole gun drilling[J]. International Journal of Machine Tools and Manufacture, 2016, 108: 66-73.

[2] KALADHAR M, SUBBAIAH K V, SRINIVASA RAO C H. Machining of austenitic stainless steels—A review[J]. International Journal of Machining and Machinability of Materials, 2012, 12(1/2): 178.

[3] KHAN S A, SHAMAIL S, ANWAR S, et al. Wear performance of surface treated drills in high speed drilling of AISI 304 stainless steel[J]. Journal of Manufacturing Processes, 2020, 58: 223-235.

[4] ARUNKUMAR N, GANESH M, RAJARAM M, et al. Deep hole drilling of AISI 1045: Effect on hole quality & tool wear under flood, emulsion, and mist cooling technique[J]. Journal of the Brazilian Society of Mechanical Sciences and Engineering, 2023, 45 (4): 195.

[5] XU Y S, ZHANG J, ZHANG Q J, et al. Theoretical and experimental investigations of tool wear in ultrasonic vibration-assisted turning of 304 austenitic stainless steel[J]. The International Journal of Advanced Manufacturing Technology, 2023, 127(7): 3157-3181.

[6] USMAN M M, ZOU P, YANG Z Y, et al. Evaluation of micro-textured tool performance in ultrasonic elliptical vibration-assisted turning of 304 stainless steel [J]. The International Journal of Advanced Manufacturing Technology, 2022, 121(7): 4403-4418.

[7] XIE C, LI L, ZHANG Y, et al. Analysis of machining quality of 304 stainless steel deep hole by changing angle of gun drill[J]. The International Journal of Advanced Manufacturing Technology, 2022, 123(1): 287-298.

[8] LI W J, ZHOU B W, XING L J, et al. Influence of cutting parameters and tool nose radius on the wear behavior of coated carbide tool when turning austenitic stainless steel[J]. Materials Today Communications, 2023, 37: 107349.

[9] SAKETI S, BEXELL U, ÖSTBY J, et al. On the diffusion wear of cemented carbides in the turning of AISI 316L stainless steel[J]. Wear, 2019, 430: 202-213.

[10] HE Q, DEPAIVA J M, KOHLSCHEEN J, et al. A study of mechanical and tribological properties as well as wear performance of a multifunctional bilayer AlTiN PVD coating during the ultra-high-speed turning of 304 austenitic stainless steel[J]. Surface and Coatings Technology, 2021, 423: 127577.

[11] LI L, HE N, WU P, et al. A gun drill mechanics model analysis based on 15-5PH solid solution stainless steel[J]. Machining Science and Technology, 2019, 23(2): 218-231.

[12] LI L, HE N, HAO X Q, et al. Deep-hole gun drilling mechanics model of Ti6Al4V alloy based on Johnson and Cook flow stress model[J]. The International Journal of Advanced Manufacturing Technology, 2019, 104(9): 4497-4508.

[13] LI L, HE N, XUE H. Chip formation mechanism of deep-hole gun drilling of Ti6Al4V titanium alloy[J]. Transactions of Nanjing University of Aeronautics and Astronautics, 2020, 37(1): 164-174.

[14] ABISHEKRAJ N, GOWTHAM T, KRISHNARAJ V, et al. Surface roughness evaluation in machining titanium alloys using non-textured and textured cutting inserts[J]. IOP Conference Series: Materials Science and Engineering, 2020, 912(3): 032076.

[15] WOSNIAK F A, POLLI M L, DE CAMARGO

BELTRÃO P A. Study on tool wear and chip shapes in deep drilling of AISI 4150 steel[J]. Society of Mechanical Sciences and Engineering, 2016, 38(2): 473-480.

Acknowledgements This work was supported by the Natural Science Research of Jiangsu Higher Education Institutions of China (No.20KJA460005), Jiangsu Postgraduate Innovation Program (No.SJCX24_2156), and Yancheng Key Research & Development (Industrial Support) Program (No.BE2023028).

Authors

The first author Mr. **JIANG Jitao** is currently a postgraduate in Department of Mechanical Engineering, Yancheng Institute of Technology, Yancheng, China. His research interests are high performance machining and deep hole processing technology and equipment.

The corresponding author Prof. **LI Liang** received the Ph.D. degree in mechanical engineering from Nanjing University of Aeronautics and Astronautics, Nanjing, China, in 2018. He is currently a professor with Department of Mechanical Engineering, Yancheng Institute of Technology. His research interests include high performance machining, deep hole processing, agricultural machinery design and equipment.

Author contributions Mr. **JIANG Jitao** designed the study, complied the models, conducted the analysis, interpreted the results, and wrote the manuscript. Prof. **LI Liang** contributed to the relationship and background of tool wear mechanism. Ms. **SHI Mengting**, Mr. **ZHOU Zilong**, and Ms. **WANG Ye** processed the experimental data. All authors commented on the manuscript draft and approved the submission.

Competing interests The authors declare no competing interests.

(Production Editor: XU Chengting)

304不锈钢深孔枪钻加工刀具磨损机理和试验研究

姜季涛，李　亮，石梦婷，周子龙，王　烨

(盐城工学院机械学院，盐城 224051，中国)

摘要：深孔枪钻加工处于封闭半封闭状态，加工过程复杂，加工中钻削力不稳定、刀具磨损严重和加工质量差一直是深孔枪钻加工的难点。304不锈钢具有良好的耐腐蚀性和耐热性，广泛应用于各行业，但是硬度高、塑性差和黏刀的特性一直制约着其在工程应用方面的发展。因此，本文以304不锈钢为研究对象，开展工艺参数优化试验和刀具磨损试验。首先，基于工艺参数优化试验，分析切削速度和进给量对钻削力和孔壁粗糙度的影响规律，优选出后续试验工艺参数为：主轴转速1 270 r/mm、进给量0.02 mm/r和油压3 MPa；其次，基于刀具磨损试验，研究刀具磨损量和刀具磨损形式变化规律，借助扫描电镜(Scanning electron microscope，SEM)和能谱仪(Energy disperse spectroscopy，EDS)，阐述深孔枪钻加工304不锈钢刀具磨损机理；最后，揭示刀具磨损对加工质量的影响规律，提出刀具重磨建议。

关键词：枪钻；304不锈钢；刀具磨损；加工质量